19. Kim J, Oh WJ, Gaiano N, Yoshida Y, Gu C: Semaphorin 3E-Plexin-D1 signaling regulates VEGF function in developmental angiogenesis via a feedback mechanism. Genes Dev 2011, 25:1399–1411
20. Nonaka H, Tanaka M, Suzuki K, Miyajima A: Development of murine hepatic sinusoidal endothelial cells characterized by the expression of hyaluronan receptors. Dev Dyn 2007, 236:2258–2267
21. Takase HM, Itoh T, Ino S, Wang T, Koji T, Akira S, Takikawa Y, Miyajima A: FGF7 is a functional niche signal required for stimulation of adult liver progenitor cells that support liver regeneration. Genes Dev 2013, 27:169–181
22. Miyaoka Y, Ebato K, Kato H, Arakawa S, Shimizu S, Miyajima A: Hypertrophy and unconventional cell division of hepatocytes underlie liver regeneration. Curr Biol 2012, 22:1166–1175
23. Reddy GK, Enwemeka CS: A simplified method for the analysis of hydroxyproline in biological tissues. Clin Biochem 1996, 29:225–229
24. Nonaka H, Sugano S, Miyajima A: Serial analysis of gene expression in sinusoidal endothelial cells from normal and injured mouse liver. Biochem Biophys Res Commun 2004, 324:15–24
25. Weddle CC, Hornbrook KR, McCay PB: Lipid peroxidation and alteration of membrane lipids in isolated hepatocytes exposed to carbon tetrachloride. J Biol Chem 1976, 251:4973–4978
26. Wanschel A, Seibert T, Hewing B, Ramkhelawon B, Ray TD, van Gils JM, Rayner KJ, Feig JE, O'Brien ER, Fisher EA, Moore KJ: Neuroimmune guidance cue Semaphorin 3E is expressed in atherosclerotic plaques and regulates macrophage retention. Arterioscler Thromb Vasc Biol 2013, 33:886–893
27. Fukushima Y, Okada M, Kataoka H, Hirashima M, Yoshida Y, Mann F, Gomi F, Nishida K, Nishikawa S, Uemura A: Sema3E-PlexinD1 signaling selectively suppresses disoriented angiogenesis in ischemic retinopathy in mice. J Clin Invest 2011, 121:1974–1985
28. Suzuki K, Tanaka M, Watanabe N, Saito S, Nonaka H, Miyajima A: p75 Neurotrophin receptor is a marker for precursors of stellate cells and portal fibroblasts in mouse fetal liver. Gastroenterology 2008, 135:270–281.e273
29. Passino MA, Adams RA, Sikorski SL, Akassoglou K: Regulation of hepatic stellate cell differentiation by the neurotrophin receptor p75NTR. Science 2007, 315:1853–1856
30. Moriya J, Minamino T, Tateno K, Okada S, Uemura A, Shimizu I, Yokoyama M, Nojima A, Okada M, Koga H, Komuro I: Inhibition of semaphorin as a novel strategy for therapeutic angiogenesis. Circ Res 2010, 106:391–398
31. Liu B, Chen Y, St Clair DK: ROS and p53: a versatile partnership. Free Radic Biol Med 2008, 44:1529–1535
32. LeCouter J, Moritz DR, Li B, Phillips GL, Liang XH, Gerber HP, Hillan KJ, Ferrara N: Angiogenesis-independent endothelial protection of liver: role of VEGFR-1. Science 2003, 299:890–893
33. Martin P, Leibovich SJ: Inflammatory cells during wound repair: the good, the bad and the ugly. Trends Cell Biol 2005, 15:599–607
34. Ishikawa K, Mochida S, Mashiba S, Inao M, Matsui A, Ikeda H, Ohno A, Shibuya M, Fujiwara K: Expressions of vascular endothelial growth factor in nonparenchymal as well as parenchymal cells in rat liver after necrosis. Biochem Biophys Res Commun 1999, 254:587–593
35. Valfre di Bonzo L, Novo E, Cannito S, Busletta C, Paternostro C, Povero D, Parola M: Angiogenesis and liver fibrogenesis. Histol Histopathol 2009, 24:1323–1341

 DOI: 10.1002/eji.201444570 Eur. J. Immunol. 2014. 44: 2638–2647

European Journal of Immunology

Mature resting Ly6C^{high} natural killer cells can be reactivated by IL-15

Ai Omi, Yutaka Enomoto, Tsuyoshi Kiniwa, Naoko Miyata and Atsushi Miyajima

Laboratory of Cell Growth and Differentiation, Institute of Molecular and Cellular Biosciences, University of Tokyo, Tokyo, Japan

Mature NK cells are heterogeneous as to their expression levels of cell surface molecules. However, the functional differences and physiological roles of each NK-cell subset are not fully understood. In this study, we report that based on the Ly6C expression levels, mature C57BL/6 murine NK cells can be subdivided into Ly6C^{low} and Ly6C^{high} subsets. Ly6C^{high} NK cells are in an inert state as evidenced by the production of lower levels of IFN-γ and granzyme B, and they exhibit poorer proliferative potential than Ly6C^{low} NK cells. In addition, adoptive transfer experiments revealed that Ly6C^{high} NK cells are derived from Ly6C^{low} NK cells in the steady state. These results strongly suggest that Ly6C^{high} NK cells are resting cells in the steady state. However, in vitro, Ly6C^{high} NK cells become Ly6C^{low} NK cells with strong effector functions upon stimulation with IL-15. Moreover, Ly6C^{high} NK cells also revert to Ly6C^{low} NK cells in vivo upon injection of the IL-15 inducers polyI:C and CpG. Taken together, these results demonstrate the plasticity of mature NK cells and suggest that Ly6C^{high} NK cells are a reservoir of potential NK cells that allow effective and strong response to infections.

Keywords: Innate immunity · Interleukin · Memory · NK cell · Viral infection

Additional supporting information may be found in the online version of this article at the publisher's web-site

Introduction

NK cells are the third most populous lymphocytes and contribute to innate immune responses as effector cells [1, 2]. NK cells are distributed throughout the body, in both lymphoid and nonlymphoid organs, for participation in immune surveillance of tumors or viral infection [1, 3, 4]. Among their various functions, NK cells play major roles in cytotoxicity and the production of inflammatory cytokines such as IFN-γ [1, 3, 4]. Unlike B and T lymphocytes, NK cells do not express a rearranged Ag-specific receptor, but express many types of activating and inhibitory receptors that recognize target cells [2–4]. Cross-linking of these receptors by their ligands regulates the functions of NK cells, and activated NK cells secrete large amounts of IFN-γ and cytotoxic granules containing perforin and granzyme B [1, 3]. Given these features, NK cells have been classified as group 1 innate lymphoid cells [5].

NK cells are differentiated from hematopoietic stem cells and develop in mainly the BM [6]. In mice, NK-cell progenitors express CD122, which is the common subunit of IL-2R and IL-15R [6]. NK cells in the early developmental stage express NK1.1 and NKG2D, followed by the expression of inhibitory and activating receptors such as those in the CD94-NKG2 family or LY49 family [6]. Thereafter, NK cells in the late developmental stage express CD11b at high levels and become mature NK cells [6]. Thus, NK cells show different expression patterns of these surface markers during development and maturation.

Mature NK cells were originally described as a homogenous cell population characterized by their ability to mediate spontaneous

Correspondence: Dr. Yutaka Enomoto
e-mail: yenomoto@iam.u-tokyo.ac.jp

cytotoxicity against target cells [7–9]. However, in the early 1980s it was proposed that human mature NK cells in peripheral blood can be subdivided into two functional subsets based on the expression of CD56 [10]. $CD56^{dim}$ and $CD56^{bright}$ NK cells exhibit clearly distinct effector functions; that is, $CD56^{dim}$ NK cells posess high cytotoxic capacity, while $CD56^{bright}$ NK cells produce a large amount of cytokines [11–13]. However, as CD56 is not expressed in mice, it has been difficult to identify functionally distinct NK-cell subsets in mice. Recently, efforts have been made to find cell surface markers that can be used to characterize mature murine NK cells and several candidate molecules such as CD27, KLRG1, and CD94 have been found. These studies revealed that mature murine NK cells can be also subdivided into subsets [14–16]. However, their functional differences and physiological roles of each subset remain elusive.

To address this question, we searched for a better marker that can be used to characterize mature NK cells. In the present study, we report that mature murine NK cells ($NK1.1^+CD11b^+CD3e^-$) can be subdivided according to their Ly6C expression levels into $Ly6C^{low}$ and $Ly6C^{high}$ subsets. Ly6C is a member of the Ly6 superfamily and is a glycosylphosphatidylinositol-anchored cell surface molecule [17]. Ly6C is expressed mainly in lymphocytes, monocytes/macrophages, granulocytes, and endothelial cells, and is a useful marker to distinguish the various developmental stages of these cells [18–20]. Moreover, it is well known that memory $CD8^+$ T cells as well as activated $CD8^+$ T cells express higher levels of Ly6C than naive cells [2, 20, 21]. Therefore, Ly6C is often used as a maker of activation and memory in T cells. Both NK cells and $CD8^+$ T cells are derived from a common lymphoid progenitor, and have many common features [2, 22]. However, the characteristics of $Ly6C^{low}$ and $Ly6C^{high}$ NK-cell subsets are not fully understood [23]. We found that there are two states in mature murine NK cells; that is, $Ly6C^{low}$ NK cells are active state and $Ly6C^{high}$ NK cells are resting, respectively. Furthermore, we herein describe the plasticity of mature NK cells.

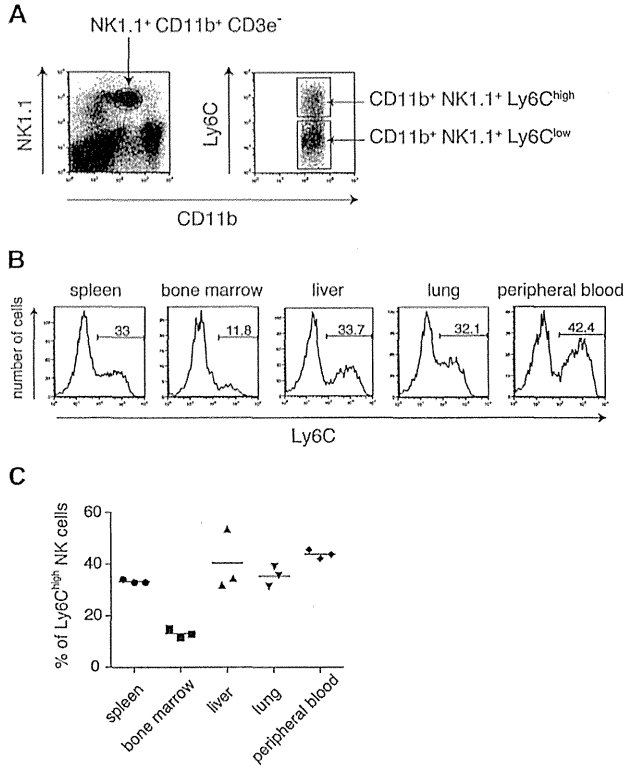

Figure 1. Ly6C expression on mature murine NK cells. (A) Cells were isolated from the spleen of C57BL/6 mice and Ly6C expression was assessed by flow cytometry. The dot plots of the right panel were gated on $NK1.1^+CD11b^+CD3e^-$ cells. (B) Cells were isolated from the spleen, BM, liver, lung, and peripheral blood of C57BL/6 mice and Ly6C expression was determined by flow cytometry, gating on $NK1.1^+CD11b^+CD3e^-$ cells. (C) The percentages of $Ly6C^{high}$ NK cells, as determined in (B), in each tissue are shown. Each symbol represents an individual mouse and bars represent the means within the groups ($n = 3$). p-value was calculated with one-way ANOVA method followed by Tukey's studentized range test to elucidate the group differences. BM versus spleen, liver, lung, peripheral blood: $p < 0.01$. (A and B) Data shown are from a single experiment representative of three independent experiments performed.

Results

Surface expression of Ly6C defines two subsets of mature murine NK cells

We found that mature murine NK cells ($NK1.1^+CD11b^+CD3e^-$) in the spleen can be subdivided into two populations based on the expression levels of Ly6C (Fig. 1A and B). Immature NK cells ($NK1.1^+CD11b^-CD3e^-CD27^+$) [24] were also subdivided by the expression of Ly6C, though the population of Ly6C-expressing cells was very small (Supporting Information Fig. 1).

To reveal the tissue distribution of the $Ly6C^{low}$ and $Ly6C^{high}$ subsets in mature NK cells in vivo, we examined the abundance of each NK-cell subset in lymphoid and nonlymphoid organs, such as the spleen, BM, liver, lung, and peripheral blood by flow cytometry (Fig. 1B). Although both $Ly6C^{low}$ and $Ly6C^{high}$ NK-cell subsets were found in various peripheral tissues, a majority of NK cells in the BM, in which NK cells develop [6], expressed Ly6C at low levels (Fig. 1B and C). These results indicate that the $Ly6C^{high}$ NK-cell subset is present mainly in peripheral tissues.

Distinct expression patterns of surface markers in NK-cell subsets

NK cells express various activating and inhibitory receptors, and their expression patterns are closely coupled to NK-cell functions [2–4]. Thus, we examined the surface expression of NK-cell receptors on $Ly6C^{low}$ and $Ly6C^{high}$ NK cells by flow cytometry (Fig. 2A and B). The expression levels of activating receptors were similar between $Ly6C^{low}$ and $Ly6C^{high}$ NK-cell subsets with the exception of Ly49H (Fig. 2A). In contrast, $Ly6C^{high}$ NK cells displayed higher proportions of cells expressing the inhibitory receptors KLRG1 and Ly49C/I than did $Ly6C^{low}$ NK cells (Fig. 2B). Conversely, the Ly49A expression levels of $Ly6C^{low}$ NK cells were slightly higher than those of $Ly6C^{high}$ NK cells (Fig. 2B). Furthermore, we investigated

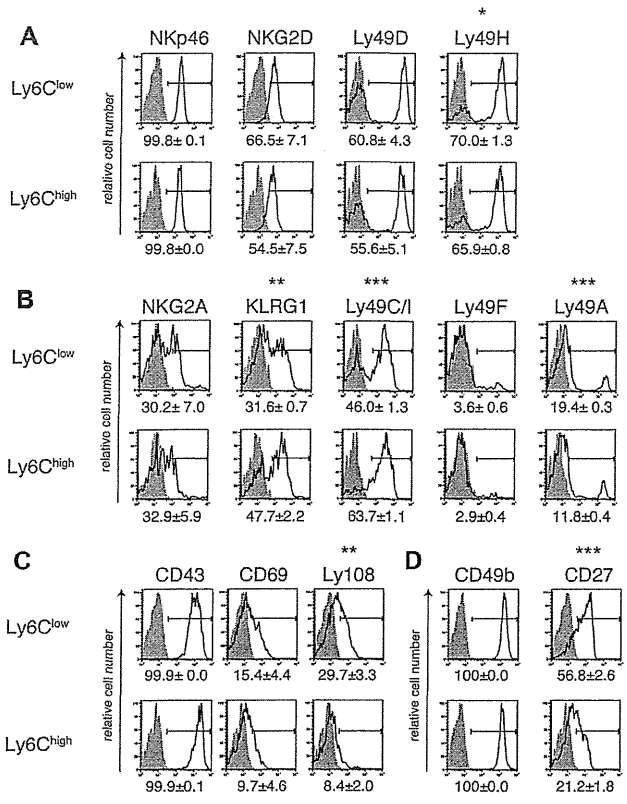

Figure 2. Characterization of surface markers on Ly6C^{low} and Ly6C^{high} NK-cell subsets. (A–D) Cells isolated from the spleens of C57BL/6 mice were stained for the indicated cell surface markers. Ly6C^{low} and Ly6C^{high} NK-cell subsets were gated on NK1.1$^+$CD11b$^+$CD3e$^-$ cells. Shaded histograms indicate isotype control. The numbers under each histogram show the mean (±SEM) percentages of positive cells for surface marker expression calculated from three mice and the histograms are representative of three independent experiments performed. $^*p < 0.05$, $^{**}p < 0.01$, $^{***}p < 0.001$ (Student's two-tailed *t*-test).

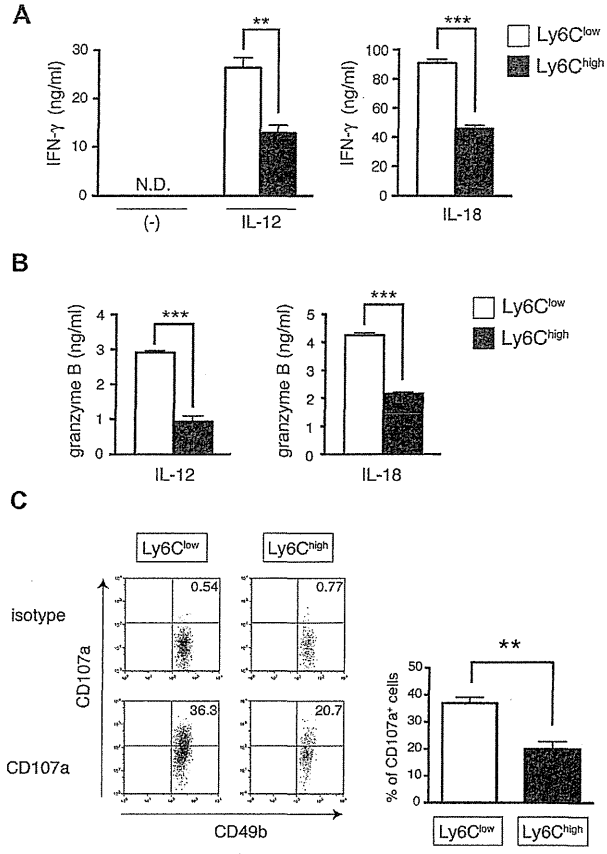

Figure 3. IFN-γ production and granzyme B secretion of Ly6C^{low} NK cells and Ly6C^{high} NK cells. (A and B) CD49b$^+$CD11b$^+$CD3e$^-$Ly6C^{low} NK cells and CD49b$^+$CD11b$^+$CD3e$^-$Ly6C^{high} NK cells were sorted from the spleens of C57BL/6 mice. Sorted NK-cell subsets (5×10^4 cells/well) were stimulated with IL-12 (100 ng/mL) or IL-18 (100 ng/mL) in the presence of IL-2 (100 ng/mL). After 24 h of incubation, the levels of (A) IFN-γ and (B) granzyme B in the culture supernatants were measured by ELISA. Data are shown as means + SEM of three samples. (C) CD49b$^+$ NK cells were cultured with IL-18 (100 ng/mL) in the presence of IL-2 (100 ng/mL). After 16 h of incubation, NK cells were cocultured with YAC-1 cells by an E:T ratio of 1:1. The dot plot represents the percentage of CD107a$^+$ cells gated on CD49b$^+$CD11b$^+$CD3e$^-$ Ly6C^{low} or Ly6C^{high} NK cells. The bar graphs represent the means (+SEM) percentages of CD107a$^+$ cells ($n = 3$). All data shown are from a single experiment representative of three independent experiments performed. $^{**}p < 0.01$, $^{***}p < 0.001$. N.D., not detected (Student's two-tailed *t*-test).

activation markers known to be upregulated in activated NK cells [25–28] and found that the expression levels of Ly108 were significantly lower in Ly6C^{high} NK cells than in Ly6C^{low} NK cells (Fig. 2C). Taken together, these results suggest that the activity of Ly6C^{high} NK cells is lower than that of Ly6C^{low} NK cells. We next examined the expression of maturation markers in NK cells, namely CD49b and CD27 [6, 14, 24]. CD49b was highly expressed in both Ly6C^{low} and Ly6C^{high} NK cells (Fig. 2D), whereas Ly6C^{high} NK cells displayed lower proportions of cells expressing CD27 than did Ly6C^{low} NK cells (Fig. 2D). This result implies that the maturation stage of Ly6C^{low}and that of Ly6C^{high} NK cells are different. While it has been known that CD27 subdivides mature murine NK cells into two populations, our results suggest that the expression of Ly6C did not match the expression of CD27 completely.

Ly6C^{high} cells are inert NK cells

NK cells have various functions in the immune system. Among them, IFN-γ production and cytotoxicity play major roles for the clearance of infectious pathogens and tumor cells [1, 3, 4]. Therefore, we next examined IFN-γ production by each NK-cell subset. NK cells are known to produce IFN-γ in response to IL-12 or IL-18, which are secreted by APCs such as DCs [1, 29]. As shown in Figure 3A, both NK-cell subsets secreted IFN-γ in response to IL-12 or IL-18. However, IFN-γ secretion by Ly6C^{high} NK cells was approximately half that of Ly6C^{low} NK cells (Fig. 3A). In order to exclude the possibility that viability of NK-cell subsets were different during the assay, IL-2 was added to maintain the survival of NK cells [30, 31]. Subsequently, there was no difference in cell viability between Ly6C^{low} and ly6C^{high} NK cells (data not shown). Activated NK cells release cytotoxic granules containing perforin and granzyme B to kill target cells [1, 3]. Granzyme

B directly cleaves caspases and activates the apoptotic-signaling pathway in target cells [32, 33]. To evaluate the cytotoxic capability of each NK-cell subset, we examined the secretion of granzyme B in response to IL-12 or IL-18. Production of granzyme B by Ly6C^{high} NK cells was lower than that by Ly6C^{low} NK cells when stimulated with IL-12 or IL-18 (Fig. 3B). In addition, we examined CD107a expression in each NK-cell subset when cocultured with YAC-1 cells. CD107a is a glycoprotein present in the membrane of cytotoxic granules and exposed on the surface of activated NK cells [34]. Consistent with granzyme B productions, the percentage of CD107a$^+$ cells in Ly6C^{high} NK cells was lower than that in Ly6C^{low} NK cells when stimulated with IL-18 (Fig. 3C). These data collectively indicate that Ly6C^{low} NK cells exhibit stronger NK functions than do Ly6C^{high} NK cells in response to cytokine stimulation. These results correlated with our finding that Ly6C^{high} NK cells express higher levels of KLRG1, Ly49C/I, and lower levels of Ly108 (Fig. 2B). Therefore, Ly6C^{high} NK cells are thought to be refractory to cytokine stimulation.

Ly6C^{low} NK cells become Ly6C^{high} NK cells in the steady state

We next investigated the interrelationship of Ly6C^{low} and Ly6C^{high} NK cells. To determine whether these NK-cell subsets are interconvertible, we performed an in vivo transplantation assay. NK-cell subsets were sorted from the spleens of CD45.2 C57BL/6J (C57BL/6) mice and adoptively transferred into nonirradiated CD45.1 congenic mice by i.v. injection. Two weeks after the transplantation, we isolated the transferred CD45.2$^+$ NK cells from the spleen and examined their expression levels of Ly6C. Approximately 30% of CD45.2$^+$ NK cells in mice that received Ly6C^{low} NK cells were Ly6C^{high}, indicating that a significant portion of the transferred Ly6C^{low} NK cells were converted to Ly6C^{high} NK cells (Fig. 4A and B). In contrast, almost all transferred Ly6C^{high} NK cells did not change their high expression levels of Ly6C (Fig. 4A and B). These results suggest that Ly6C^{low} NK cells become Ly6C^{high} NK cells, but not vice versa in the steady state.

IL-15 converts Ly6C^{high} NK cells to Ly6C^{low} NK cells

IL-15 is a major cytokine required for the development and proliferation of NK cells [31, 35, 36]. To determine whether IL-15 affects the Ly6C expression levels of NK cells, both Ly6C^{low} and Ly6C^{high} NK cells were sorted and cultured with IL-15. First, we determined the absolute cell number of Ly6C^{low} and Ly6C^{high} NK cells. After 6-day culture, both subsets survived and Ly6C^{low} NK cells showed significantly higher proliferative potential than Ly6C^{high} NK cells (Fig. 5A). Next, we examined the expression levels of Ly6C at indicated time points. The Ly6C expression levels in Ly6C^{low} NK cells remained unchanged (Fig. 5B, left panel). Interestingly, however, the Ly6C expression levels of Ly6C^{high} NK cells gradually decreased, and about a half of the NK cells expressed Ly6C at

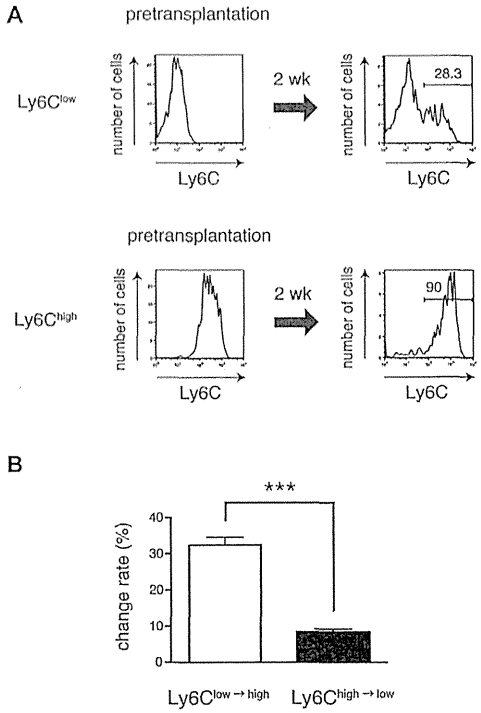

Figure 4. Ly6C^{high} NK cells are derived from Ly6C^{low} NK cells. (A and B) CD49b$^+$CD11b$^+$CD3e$^-$Ly6C^{low} NK cells and CD49b$^+$CD11b$^+$CD3e$^-$Ly6C^{high} NK cells were sorted from the spleen of CD45.2 C57BL/6 mice and transferred into nonirradiated CD45.1 congenic mice. Two weeks later, cells were harvested from the spleens of the recipient mice, stained for CD49b, CD11b, CD3e, CD45.2, and Ly6C and analyzed by flow cytometry. (A) The histogram plots show Ly6C expression profiles gated on CD49b$^+$CD11b$^+$CD3e$^-$CD45.2$^+$ cells. Numbers indicate percentage of Ly6C-positive cells. Data shown are from a single experiment representative of three independent experiments performed. (B) The graph indicates change rate of each subset (i.e., the percentage of Ly6C^{high} NK cells derived from Ly6C^{low} NK cells or Ly6C^{low} NK cells derived from Ly6C^{high} NK cells). Data shown are the means + SEM of three independent experiments performed. These data were compared using Student's two-tailed *t*-test. $^{***}p < 0.001$.

middle levels (Ly6C$^{mid(high)}$ NK cells) when cultured with IL-15 for 4 days, and finally many NK cells became Ly6C^{low} NK cells after 6 days in culture with IL-15 (Fig. 5B, right panel). Furthermore, we examined the effect of IL-2 on the expression levels of Ly6C, as IL-2 and IL-15 share the common cytokine-receptor gamma chain and IL-2 is also a major cytokine required for the development and proliferation of NK cells. After 6-day culture with IL-2, both subsets survived and Ly6C^{low} NK cells showed significantly higher proliferative capacity than Ly6C^{high} NK cells (Supporting Information Fig. 2A). Ly6C expression levels of Ly6C^{high} NK cells decreased and approximately half of the NK cells expressed Ly6C at intermediate levels (Supporting Information Fig. 2B). These results suggest that IL-2 also has the effect to convert Ly6C^{high} NK cells to Ly6C^{low} NK cells. However, the effect of IL-2 was not so strong as that of IL-15. Because the functions of the Ly6C^{low} NK cells were higher than those of the Ly6C^{high} NK cells (Fig. 3), we analyzed the effector functions of Ly6C^{low} NK cells derived from Ly6C^{low} NK cells (Ly6C$^{low(low)}$ NK cells) and of Ly6C$^{mid(high)}$ NK cells or Ly6C^{low}

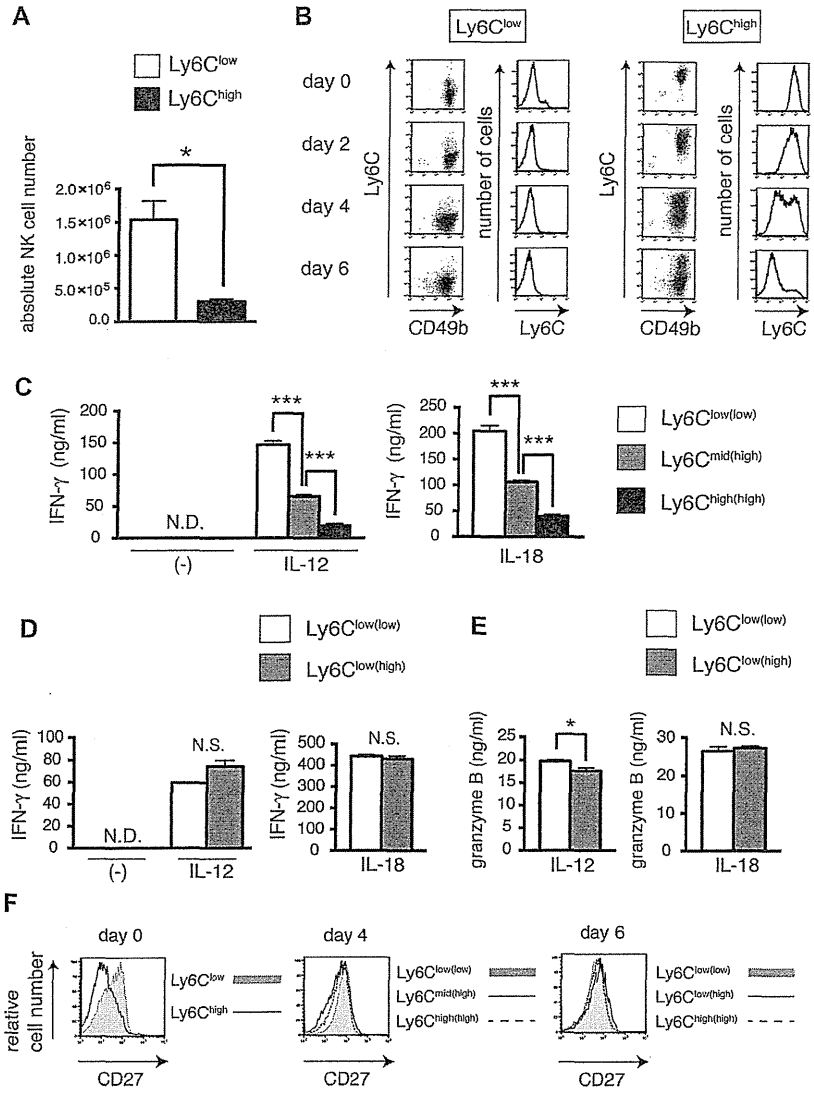

Figure 5. Conversion of Ly6C^{high} NK cells to Ly6C^{low} NK cells. (A) CD49b$^+$CD11b$^+$CD3e$^-$Ly6C^{low} NK cells and CD49b$^+$CD11b$^+$CD3e$^-$Ly6C^{high} NK cells (3×10^5) were cultured with IL-15 (100 ng/mL) for 6 days and absolute cell number was determined in triplicate cultures by using a 0.4% Trypan blue solution. Data are shown as means + SEM of three samples from a single experiment representative of three independent experiments. (B) CD49b$^+$CD11b$^+$CD3e$^-$Ly6C^{low} NK cells and CD49b$^+$CD11b$^+$CD3e$^-$Ly6C^{high} NK cells were cultured with IL-15 (100 ng/mL) for the indicated time periods. During each time period, cells were harvested and stained for CD49b, CD11b, CD3e, and Ly6C. Data shown are from a single experiment representative of three independent experiments performed. (C) NK-cell subsets were cultured with IL-15 (100 ng/mL) for 4 days. Ly6C$^{low(low)}$ NK cells, Ly6C$^{mid(high)}$ NK cells, and Ly6C$^{high(high)}$ NK cells were sorted by cell sorter and stimulated with IL-12 (100 ng/mL) or IL-18 (100 ng/mL) in the presence of IL-2 (100 ng/mL) (2×10^4 cells/well). After 24 h of incubation, the levels of IFN-γ in the culture supernatants were measured by ELISA. Data are shown as means + SEM of three samples from a single experiment representative of three independent experiments. (D, E) NK-cell subsets were cultured with IL-15 (100 ng/mL) for 7 days. Ly6C$^{low(low)}$ NK cells and Ly6C$^{low(high)}$ NK cells were then sorted and stimulated with IL-12 (100 ng/mL) or IL-18 (100 ng/mL) in the presence of IL-2 (100 ng/mL) (2×10^4 cells/well). After 24 h of incubation, the levels of (D) IFN-γ and (E) granzyme B in the culture supernatants were measured by ELISA. Data are shown as means + SEM of three samples from a single experiment representative of three independent experiments. (F) NK-cell subsets were cultured with IL-15 (100 ng/mL) for 4 or 6 days. The histogram plots show CD27 expression profiles gated on CD49b$^+$CD3e$^-$Ly6C$^{low/mid/high}$ cells. Data shown are a representative of two independent experiments. $^*p < 0.005$, $^{***}p < 0.001$. N.D., not detected, N.S., not significant (Student's two-tailed t-test).

NK cells derived from Ly6C^{high} NK cells (Ly6C$^{low(high)}$ NK cells) 4 days or 1 week in culture with IL-15, respectively. We found that the ability of Ly6C$^{mid(high)}$ NK cells to secrete IFN-γ was lower than that of Ly6C$^{low(low)}$ NK cells in response to IL-12 or IL-18 (Fig. 5C). Notably, approximately half of the Ly6C^{high} NK cells retained high expression levels of Ly6C (Ly6C$^{high(high)}$ NK cells) 4 days in culture with IL-15, and the production of IFN-γ of Ly6C$^{mid(high)}$ NK cells was higher than Ly6C$^{high(high)}$ NK cells (Fig. 5C). The ability of Ly6C$^{low(high)}$ NK cells to secrete IFN-γ and granzyme B was increased to levels comparable to that of Ly6C$^{low(low)}$ NK cells for 1 week in the presence of IL-15 (Fig. 5D and E). As stated above, Ly6C^{high} NK cells displayed lower proportions of cells expressing CD27 than did Ly6C^{low} NK cells before culture with IL-15 (Fig. 2D). We therefore examined CD27 expression levels of both Ly6C^{low} and Ly6C^{high} NK cells in culture with IL-15 for 4 days, and found no differences in the expression levels of CD27 among the three populations of Ly6C$^{low(low)}$, Ly6C$^{mid(high)}$, and Ly6C$^{high(high)}$ NK cells (Fig. 5F). Furthermore, after 6 days in culture, there was also no difference in the expression levels of CD27 among the three populations, Ly6C$^{low(low)}$, Ly6C$^{low(high)}$, and Ly6C$^{high(high)}$ NK cells. These results indicate that the expression levels of CD27 are not well correlated with activity of mature NK cells.

Conversion of Ly6C^{high} NK cells to Ly6C^{low} NK cells in vivo

We next examined whether Ly6C^{high} NK cells could become Ly6C^{low} NK cells in vivo. Because IL-15 was shown to convert Ly6C^{high} NK cells into Ly6C^{low} NK cells in vitro (Fig. 5B), we first performed an in vivo transplantation assay by overexpressing IL-15 in mice. To express IL-15 in vivo, we utilized the hydrodynamic tail vein injection method [37–39]. NK-cell subsets were sorted from the spleens of CD45.2 C57BL/6 mice and adoptively transferred into CD45.1 congenic mice injected with control vector

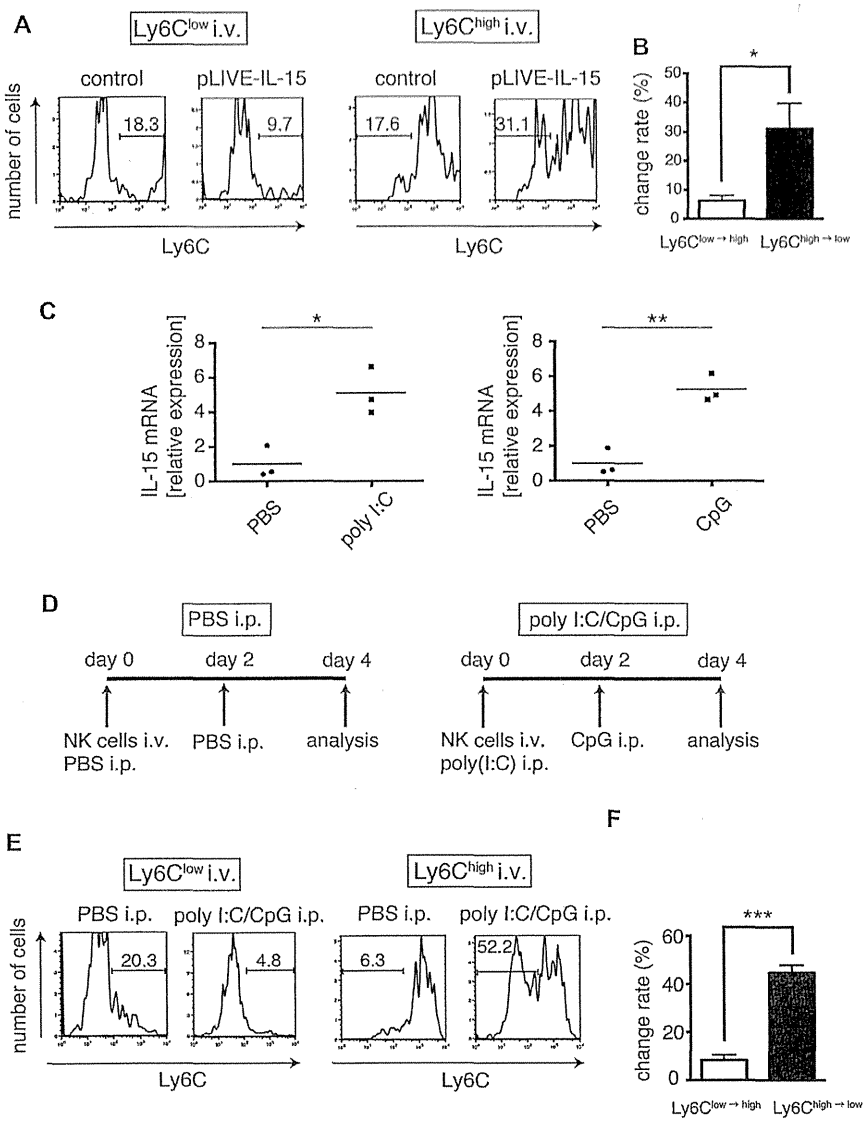

Figure 6. Conversion of Ly6C^{high} NK cells to Ly6C^{low} NK cells in vivo. (A and B) control vector or pLIVE-IL-15 (20 μg) were injected i.v. into CD45.1 congenic mice. Six hours after injection, NK-cell subsets (3×10^5 to 5×10^5cells) from the spleens of CD45.2 C57BL/6 mice were transferred into these CD45.1 mice. Four days later, cells were harvested from the spleens of the recipient mice, stained for CD49b, CD11b, CD3e, CD45.2, and Ly6C and analyzed by flow cytometry. The histogram plots show Ly6C expression profiles gated on CD49b$^+$CD11b$^+$CD3e$^-$CD45.2$^+$ cells. Numbers indicate percentages. Plots are representative of three independent experiments. (B) Change rate of each subset described in (A) ($n = 4$). (C) C57BL/6 mice were injected i.p. with PBS, 100 μg of polyI:C, or 20 nmol of CpG. After 3 h, splenocytes from these C57BL/6 mice were harvested. Expression of IL-15 mRNA was determined by real-time RT-PCR. The expression levels were normalized to HPRT. Each symbol represents an individual mouse and bars represent the means within the groups. Data are pooled from three independent experiments. (D) NK-cell subsets were sorted from the spleens of CD45.2 C57BL/6 mice and transferred into nonirradiated CD45.1 congenic mice. These mice were then injected i.p. with polyI:C (day 0) and CpG (day 2) or PBS (day 0 and day 2) ($n = 3$). Splenocytes were harvested from the recipient mice transferred with Ly6C^{low} NK cells and Ly6C^{high} NK cells. Cells were stained for CD49b, CD11b, CD3e, CD45.2, and Ly6C and assessed by flow cytometry. (E) Histograms show Ly6C expression profiles gated on CD49b$^+$CD11b$^+$CD3e$^-$CD45.2$^+$ cells. Numbers indicate percentages. (F) The graph indicates change rate of each subset in the mouse treated with both poly I:C and CpG as described in (E). Data are shown as means + SEM of three independent experiments performed. $^*p < 0.05$, $^{**}p < 0.01$, $^{***}p < 0.001$ (Student's two-tailed t-test). i.p., intraperitoneal injection, i.v., intravenous injection.

or pLIVE-IL-15 vector. Four days posttransplantation, we isolated the transferred CD45.2 NK cells from the spleen and examined their expression levels of Ly6C. Flow cytometric analysis showed that approximately 30% of the transferred Ly6C^{high} NK cells in the mouse injected with pLIVE-IL-15 were converted to Ly6C^{low} NK cells (Fig. 6A and B). In contrast, the transferred Ly6C^{high} NK cells in the mouse injected with control vector and the transferred Ly6C^{low} NK cells remained unchanged (Fig. 6A and B). We next examined the conversion during immune responses. Because DCs are known to trans-present IL-15 to NK cells when activated by viral infection or TLR ligands such as polyI:C and CpG [40–42], we evaluated the expression of IL-15 in splenocytes harvested from mice i.p. injected with polyI:C or CpG. Real-time RT-PCR analysis demonstrated that IL-15 was significantly increased in splenocytes when stimulated with polyI:C or CpG (Fig. 6C). Next, we transferred NK-cell subsets sorted from the spleens of CD45.2 C57BL/6 mice into nonirradiated CD45.1 congenic mice that had been injected i.p. with polyI:C or both polyI:C and CpG (Fig. 6D and Supporting Information Fig. 3A). Administration of both polyI:C and CpG mimics severe viral infection, and these two different TLR ligands are assumed to activate DCs synergistically [43, 44]. We then analyzed transferred NK cells in the spleen of the recipient mouse after i.p. injection of polyI:C or both polyI:C and CpG. Flow cytometric analysis indicated that approximately 30% or half of the transferred Ly6C^{high} NK cells in the mouse treated with polyI:C or both polyI:C and CpG, respectively, were converted to Ly6C^{low} NK cells (Supporting Information Fig. 3B and C and Fig. 6E and F). In contrast, the transferred Ly6C^{high} NK cells in the mouse treated with PBS and the transferred Ly6C^{low} NK cells remained unchanged (Fig. 6E and F). Collectively, these results indicate that mature NK cells can change their phenotype in response to the environment.

Discussion

In the human, mature NK cells are subdivided into two populations based on the expression levels of CD56. These two subsets, $CD56^{dim}$ and $CD56^{bright}$ NK cells, play clearly distinct roles in terms of their effector functions; that is, $CD56^{dim}$ NK cells produce low levels of IFN-γ but exhibit a high cytotoxic capacity, while $CD56^{bright}$ NK cells produce a large amount of IFN-γ but exhibit a weak cytotoxic capacity [11–13, 45]. In mice, it has been shown that mature NK cells are divided in two populations based on the CD27 expression levels and that $CD27^{low}$ NK cells are derived from $CD27^{high}$ NK cells, and exhibit lower activity than $CD27^{high}$ NK cells [14, 24]. However, the two subsets of mature NK cells in human and mouse are not the same and physiological roles of those NK subsets remain unknown. In this study, we found that mature murine NK cells are subdivided into two subsets, $Ly6C^{low}$ and $Ly6C^{high}$ NK cells, based on the expression levels of Ly6C and characterized their functions and relationship.

NK cells play major roles for host protection against infectious pathogens and tumor cells at an early stage by IFN-γ production and cytotoxicity [1, 3, 4]. We demonstrated that $Ly6C^{high}$ NK cells produced lower levels of both IFN-γ and cytotoxic granules than did $Ly6C^{low}$ NK cells, correlating with the surface phenotype of $Ly6C^{high}$ NK cells that express higher levels of inhibitory receptors. Moreover, the proliferative potential of $Ly6C^{high}$ NK cells was lower than that of $Ly6C^{low}$ NK cells when cultured with IL-15. Lower effector functions and proliferation potential suggest that $Ly6C^{high}$ NK cells are in an inert state compared with $Ly6C^{low}$ NK cells. While the frequency of $Ly6C^{high}$ NK cells in the spleen, liver, lung, and peripheral blood was almost the same, it was significantly low in the BM where NK cells derive. Moreover, adoptive transfer of each subset showed that $Ly6C^{high}$ NK cells are derived from $Ly6C^{low}$ NK cells. These results imply that $Ly6C^{high}$ NK cells in peripheral tissues are resting cells. These results are similar to the previous study showing that $CD27^{low}$ NK cells are derived from $CD27^{high}$ NK cells, and exhibit lower activity than $CD27^{high}$ NK cells [14]. However, a major finding in our study is that inert $Ly6C^{high}$ NK cells can be reactivated.

We found that $Ly6C^{high}$ NK cells can be converted to $Ly6C^{low}$ NK cells ($Ly6C^{low(high)}$ NK cells) when cultured with IL-15. The expression levels of Ly6C also decreased when cultured with IL-2, but the effect of IL-2 was not as strong as IL-15. Moreover, the ability of $Ly6C^{low(high)}$ NK cells to secrete IFN-γ and granzyme B was increased to the level comparable to that of $Ly6C^{low}$ NK cells cultured with IL-15 ($Ly6C^{low(low)}$ NK cells). This conversion of $Ly6C^{high}$ NK cells to $Ly6C^{low}$ NK cells was also shown in vivo by overexpression of IL-15 or by the administration of polyI:C and CpG, potent inducers of IL-15. These results suggest that under the steady-state conditions, $Ly6C^{low}$ NK cells with strong activity develop in the BM and become resting $Ly6C^{high}$ NK cells. However, those resting NK cells are reactivated when IL-15 expression level is increased, for example, by virus infection. Thus, the present study suggests that $Ly6C^{high}$ NK cells are a reservoir of potential NK cells that allow effective and strong response to infections.

Ly6C is known to be expressed in lymphocytes, monocytes/macrophages, granulocytes, and endothelial cells [18–20]. Although its function is not completely understood, Ly6C shows distinct expression patterns in the different developmental stages of these cells. Interestingly, naive $CD8^+$ T cells express Ly6C at low levels, but $CD8^+$ memory T cells express Ly6C at high levels [2, 20, 21]. There are many common features between NK cells and $CD8^+$ T cells [2, 22]. Both NK cells and $CD8^+$ T cells are derived from a common lymphoid progenitor, and their development and/or maintenance is regulated by IL-15. In addition, they release perforin and granzyme B in cytotoxic granules and produce a large amount of IFN-γ during viral infection or in response to proinflammatory cytokines such as IL-12. In general, $CD8^+$ memory T cells become long-lived resting cells after the first immune response and can be reactivated by encountering the same Ag [46, 47]. Considering that the functions of $Ly6C^{high}$ NK cells are suppressed in the steady state but can be reactivated by immunological stimuli, $Ly6C^{high}$ NK cells might be similar to $CD8^+$ memory T cells expressing Ly6C.

NK cells have traditionally been classified as effector cells in the innate immune system. However, a recent report showed that NK cells also possess memory function and contribute to the adaptive immune system [48, 49]. After mouse cytomegalovirus (MCMV) infection, NK cells bearing the virus-specific Ly49H receptor resided in lymphoid and nonlymphoid organs for several months [49]. These memory NK cells were reactivated, rapidly degranulated, and produced cytokines by secondary viral challenge. Interestingly, these memory NK cells showed higher expression of Ly6C. Moreover, the same group indicated that adoptive transfer of mature NK cells into lymphopenic mice resulted in the generation of long-lived NK cells [50]. These NK cells resided in both lymphoid and nonlymphoid organs for more than 6 months, retained their functionality many months after initial transfer, and responded robustly to viral infection. However, the expression levels of Ly6C of long-lived NK cells were not shown. Further studies are necessary to uncover the mechanism of differentiation of $Ly6C^{low}$ NK cells into $Ly6C^{high}$ NK cells and address whether $Ly6C^{high}$ NK cells are long-lived NK cells, memory NK cells, or their progenitors. While our results showed that different stages of NK cells are distinguishable by the Ly6C expression levels, the role of Ly6C in NK-cell function remains unknown.

In conclusion, we showed that resting $Ly6C^{high}$ NK cells are present in WT mice in the steady state, and that these $Ly6C^{high}$ NK cells can be reactivated by IL-15.

Materials and methods

Mice

WT C57BL/6J (C57BL/6) mice were purchased from CLEA Japan, Inc. CD45.1 congenic C57BL/6 mice (RBRC 00144) were provided by RIKEN BRC through the National Bio-Resource Project of the MEXT, Japan. All mice were maintained under standard

specific pathogen free (SPF) conditions and used between 10 and 14 weeks of age. The animal studies were performed according to the guidelines set by the Institutional Animal Care and Use Committee of the University of Tokyo.

Flow cytometric analysis

RBC-depleted cells were stained for the following antibodies: brilliant violet 421-conjugated anti-CD3e; FITC-conjugated anti-CD11b; PE-conjugated anti-KLRG1, Ly49H, Ly49D, Ly49A, NKG2A, NK1.1, CD45.1, and CD45.2; PE/Cy7-conjugated anti-Ly6C; biotin-conjugated anti-CD49b, CD27, NKp46, Ly108, and NKG2D; APC-conjugated streptavidin (BioLegend); PE-conjugated anti-CD3e, Ly49C/I, and Ly49F; and biotin-conjugated anti-NK1.1 (BD Pharmingen). The stained cells were analyzed using a FACS Canto II (BD Biosciences) and the FlowJo 8.8.7 software (TreeStar, Ashland, OR).

Cell culture and proliferation assay in vitro

NK cells ($CD49b^+CD11b^+CD3e^-$) were isolated from the spleens of C57BL/6 mice and further fractionated into $Ly6C^{low}$ and $Ly6C^{high}$ NK cells using a MoFlo cell sorter (Beckman Coulter). Purified $Ly6C^{low}$ and $Ly6C^{high}$ NK cells were cultured in RPMI-1640 medium containing 10% FBS, 2-ME (50 μM), HEPES (20 mM), nonessential AA, sodium pyruvate, L-Gln, and gentamycin in the presence of recombinant mouse IL-15 (100 ng/mL, eBioscience) or IL-2 (100 ng/mL, PROSPEC). Cell survival was measured in triplicate using the Trypan blue exclusion test.

ELISA

Purified murine splenic NK cells were stimulated with IL-12 (100 ng/mL, PeproTech) or IL-18 (100 ng/mL, MBL) in the presence of IL-2 (100 ng/mL, PROSPEC). After 24 h of incubation, cell-free supernatants were analyzed using an ELISA kit for IFN-γ (BD Biosciences) or granzyme B (R&D). ELISAs were performed in triplicate.

CD107a expression

NK cells ($CD49b^+$) were isolated from the spleens of C57BL/6 mice by using MACS (Miltenyi Biotec). Purified NK cells were cultured in the presence of recombinant mouse IL-2 (100 ng/mL) and IL-18 (100 ng/mL). After 16 h incubation, NK cells were stained for CD3e, CD11b, Ly6C, and CD49b. For stimulation steps, NK cells were stained for CD107a and incubated with YAC-1 cells (RCB1165 provided by RIKEN BRC through the National Bio-Resource Project of the MEXT, Japan) by an E:T ratio of 1:1 in the presence of IL-2 (100 ng/mL) and IL-18 (100 ng/mL) for 5 h at 37°C. And then, monensin solution (10 μM, BioLegend) was added during the last 4 h of the culture. Following 5 h incubation, cells were analyzed by FACS Canto II.

Adoptive cell transfer

Sorted NK cells (5×10^5 to 1×10^6 cells) from the spleens of C57BL/6 mice were injected i.v. into nonirradiated CD45.1 congenic mice. In some experiments, the mice that received NK cells were injected i.p. with polyI:C (100 μg, InvivoGen) and CpG ODN (20 nmol, Hycult Biotech) or PBS.

Overexpression by hydrodynamic tail vein injection method

Mouse IL-15 cDNA was amplified by PCR: 5′-gcgctagccacca tgaaaattttgaaaccatatatgag-3′ and 5′-cgctcgagtcaggacgtgttgatg aaca-3′, and was inserted into the NheI and XhoI sites of a pLIVE vector (Mirus, Madison, WI). pLIVE-IL-15 (20 μg) was diluted with TransIT-EE Hydrodynamic Delivery Solution (Mirus, Madison, WI) and injected i.v. into CD45.1 congenic mice. pLIVE-SEAP (secreted alkaline phosphatase) (20 μg) was used as a control [39].

Real-time RT-PCR

C57BL/6 mice were i.p. injected with PBS, polyI:C (100 μg), or CpG ODN (20 nmol). After 3 h, splenocytes from these C57BL/6 mice were harvested and total RNA was prepared using an RNeasy Mini Kit (Qiagen). The total RNA was reverse-transcribed with PrimeScript RT Master Mix (Takara Bio Ink). Quantitative real-time RT-PCR was performed on a LightCycler 480 (Roche Applied Science) using SYBR premix Ex Taq reagent (Takara Bio Ink). HPRT was used as an internal control. The sequence of primers was as follows: 5′-tctcgtgctacttgtgtttccttc-3′ and 5′-catctatccagttggcctctgtt-3′ for IL-15 and 5′-tgacactggtaaaacaat gc-3′ and 5′-tatccaacacttcgagaggt-3′ for HPRT.

Statistical analysis

Unless otherwise stated, data are shown as means ± SEM and were compared using Student's two-tailed *t*-test. A value of $p < 0.05$ was taken to indicate statistical significance. Statistical analyses were performed using GraphPad Prism (GraphPad Software, San Diego, CA).

Acknowledgments: We would like to thank Dr. Tohru Itoh for providing us with the pLIVE-SEAP vector and pLIVE-IL-15 vector.

We would also like to thanks Dr. Cindy Kok for critical reading of the manuscript. This work was supported by research grants from the Ministry of Education, Culture, Sports, Science, and Technology (MEXT) of Japan (No. 22118006), the Ministry of Health, Labour, and Welfare (MHLW) of Japan (H24-hepatitis-general-005), and the Tokyo Biochemical Research Foundation.

Conflict of interest: The authors declare no financial or commercial conflict of interest.

References

1 Vivier, E., Tomasello, E., Baratin, M., Walzer, T. and Ugolini, S., Functions of natural killer cells. *Nat. Immunol.* 2008. 9: 503–510.

2 Sun, J. C. and Lanier, L. L., NK cell development, homeostasis and function: parallels with CD8(+) T cells. *Nat. Rev. Immunol.* 2011. 11: 645–657.

3 Cerwenka, A. and Lanier, L. L., Natural killer cells, viruses and cancer. *Nat. Rev. Immunol.* 2001. 1: 41–49.

4 Yokoyama, W. M. and Plougastel, B. F., Immune functions encoded by the natural killer gene complex. *Nat. Rev. Immunol.* 2003. 3: 304–316.

5 Spits, H., Artis, D., Colonna, M., Diefenbach, A., Di Santo, J. P., Eberl, G., Koyasu, S. et al., Innate lymphoid cells—a proposal for uniform nomenclature. *Nat. Rev. Immunol.* 2013. 13: 145–149.

6 Kim, S., Iizuka, K., Kang, H. S., Dokun, A., French, A. R., Greco, S. and Yokoyama, W. M., In vivo developmental stages in murine natural killer cell maturation. *Nat. Immunol.* 2002. 3: 523–528.

7 Strowig, T., Brilot, F. and Munz, C., Noncytotoxic functions of NK cells: direct pathogen restriction and assistance to adaptive immunity. *J. Immunol.* 2008. 180: 7785–7791.

8 Herberman, R. B., Nunn, M. E. and Lavrin, D. H., Natural cytotoxic reactivity of mouse lymphoid cells against syngeneic acid allogeneic tumors. I. Distribution of reactivity and specificity. *Int. J. Cancer.* 1975. 16: 216–229.

9 Kiessling, R., Klein, E. and Wigzell, H., "Natural" killer cells in the mouse. I. Cytotoxic cells with specificity for mouse Moloney leukemia cells. Specificity and distribution according to genotype. *Eur. J. Immunol.* 1975. 5: 112–117.

10 Lanier, L. L., Le, A. M., Phillips, J. H., Warner, N. L. and Babcock, G. F., Subpopulations of human natural killer cells defined by expression of the Leu-7 (HNK-1) and Leu-11 (NK-15) antigens. *J. Immunol.* 1983. 131: 1789–1796.

11 Frey, M., Packianathan, N. B., Fehniger, T. A., Ross, M. E., Wang, W. C., Stewart, C. C., Caligiuri, M. A. et al., Differential expression and function of L-selectin on CD56bright and CD56dim natural killer cell subsets. *J. Immunol.* 1998. 161: 400–408.

12 Jacobs, R., Hintzen, G., Kemper, A., Beul, K., Kempf, S., Behrens, G., Sykora, K. W. et al., $CD56^{bright}$ cells differ in their KIR repertoire and cytotoxic features from $CD56^{dim}$ NK cells. *Eur. J. Immunol.* 2001. 31: 3121–3127.

13 Cooper, M. A., Fehniger, T. A., Turner, S. C., Chen, K. S., Ghaheri, B. A., Ghayur, T., Carson, W. E., et al., Human natural killer cells: a unique innate immunoregulatory role for the CD56(bright) subset. *Blood* 2001. 97: 3146–3151.

14 Hayakawa, Y. and Smyth, M. J., CD27 dissects mature NK cells into two subsets with distinct responsiveness and migratory capacity. *J. Immunol.* 2006. 176: 1517–1524.

15 Huntington, N. D., Tabarias, H., Fairfax, K., Brady, J., Hayakawa, Y., Degli-Esposti, M. A., Smyth, M. J. et al., NK cell maturation and peripheral homeostasis is associated with KLRG1 up-regulation. *J. Immunol.* 2007. 178: 4764–4770.

16 Yu, J., Wei, M., Mao, H., Zhang, J., Hughes, T., Mitsui, T., Park, I. K. et al., CD94 defines phenotypically and functionally distinct mouse NK cell subsets. *J. Immunol.* 2009. 183: 4968–4974.

17 Bamezai, A., Mouse Ly-6 proteins and their extended family: markers of cell differentiation and regulators of cell signaling. *Arch. Immunol. Ther. Exp. (Warsz)* 2004. 52: 255–266.

18 Jutila, M. A., Kroese, F. G., Jutila, K. L., Stall, A. M., Fiering, S., Herzenberg, L. A., Berg, E. L., et al., Ly-6C is a monocyte/macrophage and endothelial cell differentiation antigen regulated by interferon-gamma. *Eur. J. Immunol.* 1988. 18: 1819–1826.

19 Jutila, D. B., Kurk, S. and Jutila, M. A., Differences in the expression of Ly-6C on neutrophils and monocytes following PI-PLC hydrolysis and cellular activation. *Immunol. Lett.* 1994. 41: 49–57.

20 Hanninen, A., Maksimow, M., Alam, C., Morgan, D. J. and Jalkanen, S., Ly6C supports preferential homing of central memory $CD8^+$ T cells into lymph nodes. *Eur. J. Immunol.* 2011. 41: 634–644.

21 Walunas, T. L., Bruce, D. S., Dustin, L., Loh, D. Y. and Bluestone, J. A., Ly-6C is a marker of memory $CD8^+$ T cells. *J. Immunol.* 1995. 155: 1873–1883.

22 Bezman, N. A., Kim, C. C., Sun, J. C., Min-Oo, G., Hendricks, D. W., Kamimura, Y., Best, J. A. et al., Molecular definition of the identity and activation of natural killer cells. *Nat. Immunol.* 2012. 13: 1000–1009.

23 Sato, N., Yahata, T., Santa, K., Ohta, A., Ohmi, Y., Habu, S. and Nishimura, T., Functional characterization of NK1.1+Ly-6C+ cells. *Immunol. Lett.* 1996. 54: 5–9.

24 Chiossone, L., Chaix, J., Fuseri, N., Roth, C., Vivier, E. and Walzer, T., Maturation of mouse NK cells is a 4-stage developmental program. *Blood* 2009. 113: 5488–5496.

25 Moretta, A., Poggi, A., Pende, D., Tripodi, G., Orengo, A. M., Pella, N., Augugliaro, R. et al., CD69-mediated pathway of lymphocyte activation: anti-CD69 monoclonal antibodies trigger the cytolytic activity of different lymphoid effector cells with the exception of cytolytic T lymphocytes expressing T cell receptor alpha/beta. *J. Exp. Med.* 1991. 174: 1393–1398.

26 Falco, M., Marcenaro, E., Romeo, E., Bellora, F., Marras, D., Vely, F., Ferracci, G. et al., Homophilic interaction of NTBA, a member of the CD2 molecular family: induction of cytotoxicity and cytokine release in human NK cells. *Eur. J. Immunol.* 2004. 34: 1663–1672.

27 Flaig, R. M., Stark, S. and Watzl, C., Cutting edge: NTB-A activates NK cells via homophilic interaction. *J. Immunol.* 2004. 172: 6524–6527.

28 Nieto, M., Rodriguez-Fernandez, J. L., Navarro, F., Sancho, D., Frade, J. M., Mellado, M., Martinez, A. C. et al., Signaling through CD43 induces natural killer cell activation, chemokine release, and PYK-2 activation. *Blood* 1999. 94: 2767–2777.

29 Andrews, D. M., Scalzo, A. A., Yokoyama, W. M., Smyth, M. J. and Degli-Esposti, M. A., Functional interactions between dendritic cells and NK cells during viral infection. *Nat. Immunol.* 2003. 4: 175–181.

30 Kuribayashi, K., Gillis, S., Kern, D. E. and Henney, C. S., Murine NK cell cultures: effects of interleukin-2 and interferon on cell growth and cytotoxic reactivity. *J. Immunol.* 1981. 126: 2321–2327.

31 Meazza, R., Azzarone, B., Orengo, A. M. and Ferrini, S., Role of common-gamma chain cytokines in NK cell development and function: perspectives for immunotherapy. *J. Biomed. Biotechnol.* 2011. 2011: 861920.

32 Russell, J. H. and Ley, T. J., Lymphocyte-mediated cytotoxicity. *Annu. Rev. Immunol.* 2002. 20: 323–370.

33 Andrade, F., Roy, S., Nicholson, D., Thornberry, N., Rosen, A. and Casciola-Rosen, L., Granzyme B directly and efficiently cleaves several downstream caspase substrates: implications for CTL-induced apoptosis. *Immunity* 1998. 8: 451–460.

34 Alter, G., Malenfant, J. M. and Altfeld, M., CD107a as a functional marker for the identification of natural killer cell activity. *J. Immunol. Methods* 2004. 294: 15–22.

35 Ogasawara, K., Hida, S., Azimi, N., Tagaya, Y., Sato, T., Yokochi-Fukuda, T., Waldmann, T. A. et al., Requirement for IRF-1 in the microenvironment supporting development of natural killer cells. *Nature* 1998. 391: 700–703.

36 Kennedy, M. K., Glaccum, M., Brown, S. N., Butz, E. A., Viney, J. L., Embers, M., Matsuki, N. et al., Reversible defects in natural killer and memory CD8 T cell lineages in interleukin 15-deficient mice. *J. Exp. Med.* 2000. 191: 771–780.

37 Zhang, G., Budker, V. and Wolff, J. A., High levels of foreign gene expression in hepatocytes after tail vein injections of naked plasmid DNA. *Hum. Gene Ther.* 1999. 10: 1735–1737.

38 Zhang, G., Gao, X., Song, Y. K., Vollmer, R., Stolz, D. B., Gasiorowski, J. Z., Dean, D. A., et al., Hydroporation as the mechanism of hydrodynamic delivery. *Gene Ther.* 2004. 11: 675–682.

39 Inagaki, F. F., Tanaka, M., Inagaki, N. F., Yagai, T., Sato, Y., Sekiguchi, K., Oyaizu, N. et al., Nephronectin is upregulated in acute and chronic hepatitis and aggravates liver injury by recruiting CD4 positive cells. *Biochem. Biophys. Res. Commun.* 2013. 430: 751–756.

40 Lucas, M., Schachterle, W., Oberle, K., Aichele, P. and Diefenbach, A., Dendritic cells prime natural killer cells by trans-presenting interleukin 15. *Immunity* 2007. 26: 503–517.

41 Eidenschenk, C., Crozat, K., Krebs, P., Arens, R., Popkin, D., Arnold, C. N., Blasius, A. L. et al., Flt3 permits survival during infection by rendering dendritic cells competent to activate NK cells. *Proc. Natl. Acad. Sci. USA* 2010. 107: 9759–9764.

42 Stonier, S. W. and Schluns, K. S., Trans-presentation: a novel mechanism regulating IL-15 delivery and responses. *Immunol. Lett.* 2010. 127: 85–92.

43 Napolitani, G., Rinaldi, A., Bertoni, F., Sallusto, F. and Lanzavecchia, A., Selected Toll-like receptor agonist combinations synergistically trigger a T helper type 1-polarizing program in dendritic cells. *Nat. Immunol.* 2005. 6: 769–776.

44 Zhu, Q., Egelston, C., Vivekanandhan, A., Uematsu, S., Akira, S., Klinman, D. M., Belyakov, I. M. et al., Toll-like receptor ligands synergize through distinct dendritic cell pathways to induce T cell responses: implications for vaccines. *Proc. Natl. Acad. Sci. USA* 2008. 105: 16260–16265.

45 Caligiuri, M. A., Human natural killer cells. *Blood* 2008. 112: 461–469.

46 Kaech, S. M., Tan, J. T., Wherry, E. J., Konieczny, B. T., Surh, C. D. and Ahmed, R., Selective expression of the interleukin 7 receptor identifies effector CD8 T cells that give rise to long-lived memory cells. *Nat. Immunol.* 2003. 4: 1191–1198.

47 Wherry, E. J. and Ahmed, R., Memory CD8 T-cell differentiation during viral infection. *J. Virol.* 2004. 78: 5535–5545.

48 O'Leary, J. G., Goodarzi, M., Drayton, D. L. and von Andrian, U. H., T cell- and B cell-independent adaptive immunity mediated by natural killer cells. *Nat. Immunol.* 2006. 7: 507–516.

49 Sun, J. C., Beilke, J. N. and Lanier, L. L., Adaptive immune features of natural killer cells. *Nature* 2009. 457: 557–561.

50 Sun, J. C., Beilke, J. N., Bezman, N. A. and Lanier, L. L., Homeostatic proliferation generates long-lived natural killer cells that respond against viral infection. *J. Exp. Med.* 2011. 208: 357–368.

Full correspondence: Dr. Yutaka Enomoto, Laboratory of Cell Growth and Differentiation, Institute of Molecular and Cellular Biosciences, The University of Tokyo, 1-1-1 Yayoi, Bunkyo-ku, Tokyo 113-0032, Japan
Fax: +81-3-5841-8475
e-mail: yenomoto@iam.u-tokyo.ac.jp

Additional correspondence: Dr. Atsushi Miyajima, Laboratory of Cell Growth and Differentiation, Institute of Molecular and Cellular Biosciences, The University of Tokyo; 1-1-1 Yayoi, Bunkyo-ku, Tokyo 113-0032, Japan
e-mail: miyajima@iam.u-tokyo.ac.jp

Received: 16/2/2014
Revised: 9/6/2014
Accepted: 1/7/2014
Accepted article online: 3/7/2014

Title:

Adaptive Remodeling of the Biliary Architecture Underlies Liver Homeostasis

Author names:

Kota Kaneko, Kenji Kamimoto, Atsushi Miyajima, and Tohru Itoh

Keywords:

Bile duct; Liver progenitor cells; Injury; Regeneration; Tissue plasticity

This article has been accepted for publication and undergone full peer review but has not been through the copyediting, typesetting, pagination and proofreading process which may lead to differences between this version and the Version of Record. Please cite this article as doi: 10.1002/hep.27685

FOOTNOTE PAGE

Contact Information (Corresponding Author):

Tohru Itoh, Ph.D.

Laboratory of Cell Growth and Differentiation, Institute of Molecular and Cellular Biosciences, The University of Tokyo.

1-1-1 Yayoi, Bunkyo-ku, Tokyo 113-0032, Japan

Tel. +81-3-5841-7889 Fax. +81-3-5841-8475

E-mail: itohru@iam.u-tokyo.ac.jp

List of Abbreviations:

LPCs, liver progenitor cells; BECs, biliary epithelial cells; FGF7, fibroblast growth factor 7; DDC, 3,5-diethoxycarbonyl-1,4-dihydrocollidine; CDE, choline-deficient, ethionine-supplemented diet; CCl_4,, carbon tetrachlodide; TAA, thioacetamide; BABB, benzyl benzoate:benzyl alcohol; 3D, three-dimensional; CK19, cytokeratin 19; 2D, two-dimensional; TWEAK, tumor necrosis factor-like weak inducer of apoptosis; EpCAM, epithelial cell adhesion molecule.

Financial Support:

This work was supported in part by Japan Society for the Promotion of Science (JSPS) KAKENHI Grant Numbers 22118006 (A.M.), 24112507 (T.I.), 24590342 (T.I.), and 26253023 (A.M.) as well as by CREST from Japan Science and Technology Agency (A.M.). K. Kaneko is a Research Fellow at JSPS.

ABSTRACT

Background: Serving as the center for metabolism and detoxification, the liver is inherently susceptible to a wide variety of damage imposed by toxins or chemicals. Induction of cell populations with biliary epithelial phenotypes, which include progenitor-like cells and are referred to as liver progenitor cells (LPCs), is often observed in histopathological examinations of various liver diseases in both human patients and animal models and has been implicated in regeneration. However, the tissue dynamics underlying this phenomenon still remains largely unclear.

Results: We have developed a simple imaging technique to reveal the global and fine-scale architecture of the biliary tract spreading in the mouse liver. By using this novel method, we show that emergence and expansion of LPCs actually reflect structural transformation of the intrahepatic biliary tree in mouse liver injury models. The biliary branches expanded their area gradually and contiguously along with the course of chronic injury. Relevant regulatory signals known to be involved in LPC regulation, including fibroblast growth factor 7 and tumor necrosis factor-like weak inducer of apoptosis, can modulate the dynamics of the biliary epithelium in different ways. Importantly, the structural transformations of the biliary tree were diverse and well corresponded to the parenchymal injury patterns. That is, when chronic hepatocyte damage was induced in the peri-central area, the biliary branches exhibited an extended structure from the peri-portal area with apparent tropism toward the distant injured area.

Conclusion: The hepatobiliary system possesses a unique and unprecedented structural flexibility and can remodel dynamically and adaptively in response to various injury conditions. This type of tissue plasticity should constitute an essential component to maintain liver homeostasis.

(267 words; MAX 275 words)

The liver is a vital organ that functions as the primary center for detoxification and metabolism, receiving the portal blood flowing from the intestine and abdominal viscera. It is therefore predisposed to incurring various types of injuries caused by chemicals, toxins, or metabolic disorders. Thus, the liver has presumably evolved its renowned high regenerative capacity to counter these varied injuries, thereby serving as a unique model to study tissue dynamics in response to the variety of injury.

Liver regeneration can usually be achieved without the activation of stem/progenitor cells, because mature hepatocytes exempt from damage can proliferate quickly and dominantly to replenish the lost tissue. When a persistent and intolerable level of damage compromises and disables proliferative capacity of the hepatocytes, however, putative liver stem/progenitor cells are supposed to be activated and contribute to regeneration (1, 2). Based on histopathological examinations using tissue sections, it has been well documented for decades that ectopic biliary marker-positive cells with progenitor-like phenotypes are often observed in severely and/or chronically injured liver of both human patients and rodent models. Being referred to as oval cells, atypical ductular cells, or hepatic/liver progenitor cells (LPCs), they emerge and expand from the peri-portal region to the parenchymal area, a phenomenon also known as ductular reaction. LPCs are considered to include cells with bi-lineage differentiation capability to hepatocytes and biliary epithelial cells (BECs), thereby contributing to regeneration of the damaged liver epithelia (1, 3-5). To avoid possible confusion with the terminology, it should be noted here that the term LPCs, or progenitor cells, is used by original definition, and in a strict sense, to describe only those cells with bi-lineage differentiation capability. In the meantime, however, this functional property can so far be examined and defined only under the *in vitro* culture conditions using separated cell

preparations, and there is still no marker or methodology available that can clearly distinguish these genuine functional progenitor cells from the others within the liver tissue structure. Thus, many studies involving histological analyses rather often use the same terminology to collectively describe all the ectopic biliary marker-positive cells including heterogeneous populations, regardless of their functional characteristics, which is also the case in this manuscript.

Although it is still not formally demonstrated, or rather being negated by several recent studies (6-8), whether LPCs play an exact role as a source producing new hepatocytes and/or BECs under liver injury condition, several lines of evidence support the notion that they do play a beneficial role in the regenerative process. It has been shown that the degree of the LPC expansion and ductular reaction directly correlates with severity of liver disease in human patients (9), implying its relevant role in liver pathogenesis and regeneration. Mice lacking fibroblast growth factor 7 (FGF7) or the hepatocyte growth factor receptor c-Met have a defect in inducing LPCs in a mouse model of chronic liver injury and show concomitantly elevated liver damage and decreased survival (10, 11), suggesting that the LPC induction is not just an incidental tissue malformation that occurs secondary to injuries but rather an active and adaptive homeostatic response against injury.

Despite its pathophysiologically relevant role in liver injury and regeneration, the nature of the LPC response is not fully understood yet. In particular, it still remains unclear how LPCs emerge and expand to the parenchymal area. LPCs share many common markers with BECs, and some previous studies have interpreted their appearance as migration and invasion of isolated BECs (10, 12) or ectopic production in distant areas by cell type conversion from hepatocytes (13). Meanwhile, the fact that LPCs can be

observed in tissue sections occasionally as clusters of cells with lumen-like structures also implies their structural and histological relationship with bile ducts. However, whether those clusters of LPCs are connected with each other or to the pre-existing bile duct remains to be elucidated.

Here, we show that LPCs indeed form contiguous tubular structure connected to the pre-existing bile duct and together constitute a united conduit system. By developing a novel method for visualizing the global as well as fine-scale architecture of the mouse biliary tree, we found that the emergence and expansion of LPCs actually reflected structural transformation of the biliary tree. With this new approach, we extended our analysis to the dynamics of the biliary architecture in response to various types of liver injuries, which succeeded in unveiling the hitherto unrecognized structural plasticity of the biliary epithelial tissue that underlies liver homeostasis.

Materials and Methods

Animals and liver injury models

Wild-type C57BL/6J mice were purchased from CLEA Japan, Inc. All animals were maintained under standard specific-pathogen free conditions. The experiments were performed according to the guidelines set by the institutional animal care and use committee of the University of Tokyo. For injury models, mice were fed a 0.1% 3,5-diethoxycarbonyl-1,4-dihydrocollidine (DDC)-containing diet (F-4643; Bio-serv) for the DDC model or a choline-deficient diet (MP Biomedicals) supplemented with 0.165% (wt/vol) ethionine (E5139; Sigma-Aldrich) in drinking water for the choline-deficient, ethionine-supplemented diet (CDE) model, repeatedly injected with

carbon tetrachlodide (CCl_4: 039-01276; Wako; 1 mL/kg body weight, intraperitoneally, 2 times per wk for 4 wk) for the CCl_4 model, or supplemented with thioacetamide (TAA: 204-00881; Wako; 300 mg/L) in drinking water for the TAA model. DDC treatment spanned 8 wk (Figure 2) or 3 wk (Figures 4A and 4B), CDE treatment spanned 3 wk, CCl_4 treatment spanned 4 wk, and TAA treatment spanned 4 wk (Figures 4G, 4H and 5E) or 8 wk (Figure 4K).

Visualization of the biliary tree

In order to perform the biliary tree visualization, we first set out to test several different types of inks available at the University of Tokyo CO-OP store (Bunkyo-ku, Tokyo, Japan). Pilot experiments led us to find a black waterproof fountain pen ink, SPC-200 (PLATINUM JAPAN), suitable for the visualization. The main component of this ink is "carbon black," fine particles of amorphous carbon. Fine glass capillaries were manually made by stretching microhematocrit capillary tubes (22-362-566; Fisher Scientific) heated over a gas burner. Adult mice were euthanized by cervical dislocation and subjected to laparotomy, and the ink was slowly infused to the intrahepatic biliary tract by retrograde injection from the extrahepatic bile duct using the glass capillary. In this process, fine particles of the carbon black fill the biliary tree, while the solvent is likely to leak out to the blood vessels. We infer that it mainly leaks into the portal vein, based on the injection of colored solvent (data not shown). The injection was stopped just before the ink reached the surface of the liver: excess injection leads to carbon particles leaking into the portal vein, and if further injected, into the parenchyma; the optimum amount of the ink depends on the amount of carbon particles but not on the

amount of the solvent; typically, about 15-20 μl of undiluted ink was injected for normal liver in 8-12-week-old mice. After filling the biliary tree with ink, the liver was harvested and subjected to gradual dehydration by ascending concentration series of ethanol in PBS. The applied concentration steps were 10 Vol%, 40 Vol%, and 80 Vol%, with each incubation time being one hour. The liver was finally incubated in 100% ethanol for overnight, and then soaked in a 2:1 benzyl benzoate:benzyl alcohol (BABB) solution. In BABB solution the dehydrated liver becomes optically transparent within a day or two. After clearing, the liver was imaged with microscopes (Axio Observer.Z1, Zeiss and MZ16, Leica). Three or more mice with successful ink injection were analyzed for each injury model, time point, or gene overexpression.

Sections were made and immunostained after the ink injection and even after the optical clearing. For immunostaining after the optical clearing, the cleared liver in BABB solution was applied to the inverse process of the clearing (i.e., the liver was washed with ethanol for 2 hours 3 times and incubated in ethanol for overnight to replace BABB in the tissue with ethanol, washed with PBS for 2 hours 3 times, and then incubated in PBS for overnight) to rehydrate, followed by the standard processes of cryosectioning and immunohistochemistry described in the online supporting material to check the association of the ink with the biliary marker.

Statistical analysis

Data are expressed as the mean ± standard error of the mean (SEM). The results were assessed using unpaired Student *t* test, 2-tailed. Differences were considered statistically significant when the *P* value was less than 0.05.